

RESEARCH

Open Access



# Preparation and evaluation of pirfenidone loaded chitosan nanoparticles pulmonary delivery for idiopathic pulmonary fibrosis

Kiran Dudhat<sup>1,2\*</sup>  and Harsha Patel<sup>3</sup>

## Abstract

**Background:** Idiopathic pulmonary fibrosis (IPF) is a chronic and fatal disorder caused by abnormal extracellular matrix deposition, which results in increasing dyspnea and loss of pulmonary function. Pirfenidone (PFD) has anti-fibrotic properties that have been approved by the US FDA for the treatment of IPF. Pirfenidone is currently delivered orally, which has drawbacks like reduced bioavailability in the presence of food, gastrointestinal (dyspepsia and anorexia), and dermatological (photosensitivity) side-effects, large amount of dose, and elimination half-life of 2.4 h. This study aimed was to prepare inhalable powders containing PFD-loaded chitosan nanoparticles for sustained delivery of the drug to the lung.

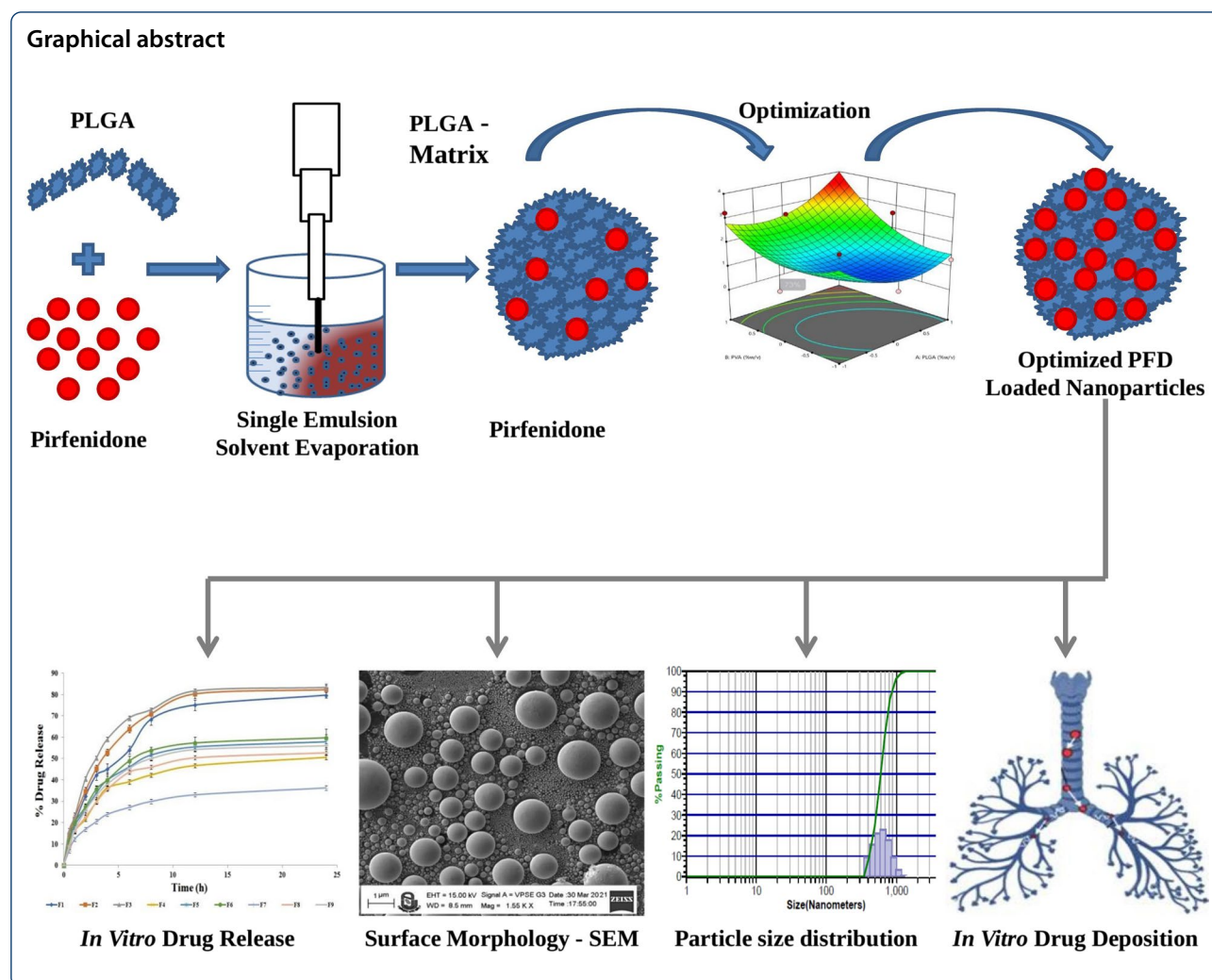
**Result:** The quasi-solvent diffusion method was used with optimized 100 mg PFD and 100 mg chitosan (CS). An *in-vitro* drug release research found that increasing the amount of chitosan reduced the rate of drug release from nanoparticles. Entrapment of PFD into chitosan nanoparticles decreased with the increased concentration of stabilizer concentration. All batches produced nanoparticles with a spherical morphology confirmed by SEM and sizes ranging from  $239.3 \pm 1.8$  to  $928.7 \pm 4.6$  nm. The optimized nanoparticles exhibited a mean particle size of  $467.33 \pm 7.8$  nm with a polydispersity index of  $0.127 \pm 0.022$ , zeta potential of  $+34.8 \pm 1.6$  mV, % entrapment efficiency ( $39.45 \pm 4.63\%$ ), % drug release after 12 h ( $94.78 \pm 2.88\%$ ), and *in-vitro* deposition (81.49%). Results showed that the obtained powders had different aerosolization properties. The particle size of nanoparticles reduced, and the process yield, extra-fine particle fraction, geometric standard diameter, and fine particle fraction increased significantly. Stability study showed, there are no aggregation observed and stable for six month study.

**Conclusion:** Prepared pirfenidone-loaded chitosan nanoparticles can be result of 6 months of stability studies that give details that there was no significant aggregation of PFD-loaded CS NPs and the spherical shape particle with smooth surface as per SEM studies. Hence, PFD-loaded CS NPs can be a suitable alternative to the currently available therapy.

**Keywords:** Chitosan, Idiopathic pulmonary fibrosis, Nanoparticles, Pirfenidone, Pulmonary drug delivery

\*Correspondence: [kichupatel@gmail.com](mailto:kichupatel@gmail.com); [Kiran.dudhat@rku.ac.in](mailto:Kiran.dudhat@rku.ac.in)

<sup>1</sup> Department of Pharmaceutics, School of Pharmacy, R K University, Kasturbadham, Rajkot, Gujarat 360020, India  
Full list of author information is available at the end of the article



## Background

Idiopathic pulmonary fibrosis (IPF) affects hundreds of millions of people around the world, lowering their quality of life and causing mortality from respiratory failure within a few years of diagnosis. IPF is a progressive lung disease that usually gets worse over time [1, 2]. This disease cannot be completely cured if it has damage to the lungs. Early recognition and diagnosis, on the other hand, can help keep this disease under control. Over time, it produces scarring in the lungs. As a result, people have trouble breathing. Even at rest, it can induce shortness of breath. Treatment options are limited, with only two FDA-approved medications available in the United States, neither of which cures the disease's lung damage or extends the lives of IPF patients [3, 4]. Exposure to hazardous elements such as coal dust, silica dust, asbestos fibers, and hard metal dust, among others, can induce lung fibrosis. [1, 5] However, in the majority of cases, the doctor is unable to identify the

particular etiology of the disease. That's why idiopathic pulmonary fibrosis is the name given to this condition.

The typical survival time from diagnosis to death is less than three years, and the incidence and mortality of IPF are increasing. Although the genesis and course of IPF have been partially recognized, there have been no therapeutic medications to treat the disease for decades [6, 7]. Currently, the medications in use (such as azathioprine and N-acetyl cysteine) are ineffective since they result in greater mortality rates and no improvement in lung function decline [8]. Pirfenidone (PFD) is the first antifibrotic agent and one of two orphan drugs approved by the USFDA in 2014 for the treatment of mild to moderate IPF [9, 10].

Pirfenidone (5-methyl-1-phenyl-2-[1H]-pyridone) is an orally administered pyridine compound and synthetic molecule. It's a non-hygroscopic white to pale yellow powder with an aqueous solubility that's too high at 25 °C. PFD may have problems with drug

delivery because it has a short half-life in the body (2.4 h), absorbs slowly after oral administration, and is primarily eliminated through urine (80 to 85%) [11, 12]. The recommended daily dose of PFD for IPF was found to be 2403 mg/day (3 tablets of 267 mg three times a day) with food, but this high amount of PFD has numerous side effects. Patients who received 2403 mg of pirfenidone per day, in Phase 3 studies had a greater rate of photosensitivity responses found at 9% [13].

Conventional formulation available in the market is tablet and capsule form with limitations like low oral route absorption due to the presence of food, faster elimination, short half-life, and potent photo-toxicity.

In pulmonary drug delivery systems, various types of nanoparticles have been utilized. Because of their particular features, polymer-based systems may be the best candidate among them [14]. Chitosan (CS) is a very effective and attractive natural polymer that has received much attention in drug delivery systems. CS is a cationic polysaccharide, comprising (1 → 4)-2-amino-2-deoxy-β-D-glucan. Chitin is the most abundant natural amino polysaccharide, and CS is the N-deacetylated derivative of it. Chitosan is a non-toxic, biocompatible, and biodegradable natural polymer with good mucoadhesive and membrane permeability-enhancing capabilities due to its cationic nature [15, 16].

In this study, PFD-loaded chitosan nanoparticles were prepared by quasi emulsion solvent evaporation method. Controlling the rate of drug release, prolonging the duration of therapeutic benefits, and delivering the drug to specific areas in the body are all being investigated with chitosan-based nanoparticles [17, 18]. The size, surface morphology and in vitro deposition behavior of dried powders were investigated. Also, in vitro drug release, aerodynamic properties and stability study from chitosan nanoparticles were examined. The nanoparticles are required small enough to be delivered deep into the lungs.

## Methods

### Materials

Low molecular weight chitosan was gifted by Meck Pharmaceuticals & Chemicals Private Limited, Gujarat, India. Pirfenidone drug was gifted by ZCL Chemicals Ltd., Gujarat, India. Polyvinyl alcohol (PVA) (90% hydrolyzed, average Mol. wt. 45,000) was supplied by Sigma Aldrich–Merck, Karnataka, India. Inhalable grade lactose was procured from Molychem, Mumbai, India. Phosphate buffer saline (PBS) pH 7.4 was obtained from Sigma–Aldrich, India. Dichloromethane and Acetic Acid (glacial) were purchased from Chemdyes Corporation, Gujarat, India. All the solvents used were of HPLC grade and other chemicals used were of analytical grade.

### Preparation of aqueous phase

In acidic environments, chitosan dissolves completely. In the composition of Chitosan nanoparticles, 4% of Acetic acid was added to the chitosan to formulate the solution. Because Pirfenidone and Chitosan both dissolve in Acetic acid, a proportion of 4 percent v/v was chosen. Initially, the volumes of acetic acid and PVA solutions were set at 5 ml and 15 ml, respectively [19, 20]. For the preparation of 20 ml of an aqueous phase, the chitosan dissolve in 5 ml of 4% acetic acid and added this soluble chitosan into the 15 ml of 1% PVA solution of magnetic stirrer.

### Preparation of PFD-loaded chitosan nanoparticles

The quasi-emulsion Solvent Evaporation Method was used to prepare CS NPs loaded with pirfenidone [21]. The 100 mg of PFD dissolved in 5 ml of dichloromethane (DCM) was taken as an organic Phase. Chitosan was dissolved in different amounts 50, 100, 150, 200, 250, and 300 mg of CS in a stabilizer solution (20 ml of 1% w/v aqueous solution of polyvinyl alcohol) with 4% acetic acid taken as an aqueous phase. Afterward, the PFD solution was added dropwise into a 20 ml CS solution (4% acetic acid) with PVA (1%) in a 100 ml flask with stirring at 400 RPM. This was followed by sonicated in a Probe Sonicator (Delta, Gujarat, India) for 1 min (220 W, 2 s/cycle). After sonication, the produced CS quasi emulsion was then stirred overnight in an uncovered beaker to allow for the evaporation of DCM. The resultant nanoparticle suspension was centrifuged at 15,000 RPM for 10 min in a cooling centrifuge (Remi, Mumbai) twice and two washing cycles were performed to the removal of traces of solvent. Finally, the prepared nanoparticles were pre-freezed in a Glycol Bath and subsequently lyophilized using a Lyophilizer (Delvac Pumps Pvt. Ltd., Chennai, India) at –79 °C for 24 h using mannitol as a cryoprotectant. The solid nanoparticles were collected after lyophilization and filled in the vial for further use [22].

### Selection of chitosan concentration in the organic phase

The pirfenidone nanoparticles were prepared using polymer chitosan with the volume ratio of organic and water phases was 1:4, and the PVA concentration in the aqueous phase was 1% [23]. The polymer concentration is varied from 50 to 400% (w/v). This study was evaluated on the bases of particle size. The CS concentration was made a direct effect on particle size. CS concentration increases, and the viscosity of aqueous phase increases during the emulsification which would produce a compact polymer matrix with larger particle size.

### Selection of PVA concentration in the aqueous phase

The pirfenidone nanoparticles were prepared using polymer chitosan; the volume ratio of organic and water phases was 1:4; the polymer amount (100 mg) is in 4% acetic acid. The PVA concentrations were variant the entrapment efficiency and particle size of pirfenidone in the chitosan nanoparticles. PVA is used as a surfactant and stabilizer both. The formulation was affected by the amount of PVA adsorbing at the polymer (chitosan) -organic solvent (DCM) -water interface. The PVA concentration in the aqueous phase from 0.5 to 2% (w/v) is varied [24].

### Characterization of the pirfenidone NPs

#### Standard curve of pirfenidone

Initially, standard curves of Pirfenidone were obtained in distilled water, methanol, dichloromethane, ethyl acetate, and phosphate buffer saline pH 7.4 in the range of 10 µg/ml to 50 µg/ml. Accurately weighed 100 mg of pirfenidone was transferred into a 100 ml volumetric flask, dissolved and diluted up to the mark with mobile phase to obtain a stock solution containing 1.0 mg/ml of pirfenidone. Aliquots from the stock solution were diluted with mobile phase to get the calibration standard solutions. Calibration standards were analyzed by UV-Visible spectrophotometer (Shimadzu UV-1800 spectrophotometer, Japan) at 311 nm ( $\lambda_{\max}$ ). Shimadzu UV Probe 2.42 software was used for Spectrophotometric analysis of pirfenidone samples. This study was conducted in triplicate and the average of the three values was recorded. The calibration curve was made by plotting the absorbance of pirfenidone against respective concentrations. The calibration curve was constructed by plotting the peak area of pirfenidone against respective concentrations [25, 26]. It gives the absorption maxima ( $\lambda_{\max}$ ) which were used to determine the amount of PFD in the in vitro dissolution sample and drug entrapped in a polymer (chitosan) matrix.

### Drug-Excipient compatibility studies

#### Fourier-transform infrared spectroscopy (FTIR) spectroscopy studies

FTIR spectra obtained from Shimadzu IR spectrophotometer (FTIR-8300), Japan equipment were used to determine the chemical stability and compatibility of the drug with the excipient. By combining with potassium bromide and pressing at 1 ton/unit, FTIR spectra of the PFD, PFD with Chitosan, and the final optimized formulation of CS NPs were obtained. FTIR spectra were scanned in the 4000–400  $\text{cm}^{-1}$  range.

### Differential scanning calorimetry (DSC) analysis studies

In a clean and dried glass mortar and pestle, samples were prepared: one was a pure drug, and the other was a physical mixture of PFD and Chitosan. Thermograms were taken with a Shimadzu (DSC-60) instrument, which was warmed at a constant rate of 10 °C/min over a temperature range of 40–300 °C. Nitrogen gas was purged at a rate of 20 ml/min to keep up in an inert environment.

### Particle size, zeta potential

A nanoparticle size analyzer was used to determine the particle size and polydispersity index (PDI) of chitosan NPs of PFD by using Zetatract 10.6.2 Instrument (Microtrac Inc., USA). To determine the total mean diameter of chitosan NPs of PFD, freshly prepared NPs dispersion (containing 1% w/v nanoparticles) were dispersed in ethanol and sonicated for 2 min, and the particle size, as well as the zeta potential, were analyzed using a Zetatract. The charged particles are oscillated using a high-frequency AC electric field. The modulated power spectrum (MPS) technique is used to examine the brownian motion power spectrum, which is a component of the power spectrum originating from oscillating particles. PFD NPs dispersion with appropriate obscuration was created, and mean particle size and zeta potential were determined in triplicate.

### Surface morphology

The surface morphology of chitosan NPs of pirfenidone was investigated. Scanning electron microscopy (SEM) was used to analyze the form and surface morphology. The samples were sputter-coated with gold and examined for morphology at a high magnification of 1.02 K X and 511 K X of pirfenidone NPs and raw pirfenidone drug respectively with an acceleration voltage of 15.0 kV. It was estimated as the mean of 300 particles measurement ( $n=300$ ).

### % Entrapment efficiency

The amount of untrapped pirfenidone recovered in the supernatant following centrifugation of the resulting nanosuspension was used to determine entrapped pirfenidone in the PFD NPs. The nanoparticles were weighed, and rinsed with distilled water; centrifuged at 15,000 RPM for 10 min at 10 °C, and the supernatant was collected. A UV-visible spectrophotometer (UV-1700 Pharma Spec, Shimadzu) was used to test the untrapped drug present in the supernatant at 311 nm. The total amount of the drug and the untrapped drug in the supernatant was calculated by percentages of entrapment efficiency (EE) using the below equation.

$$\% \text{ EE} = \frac{\text{Total amount of PFD added} - \text{Free PFD in supernatant}}{\text{Total amount of PFD added}} \times 100$$



### Yield of nanoparticles

The total weight of formulated nanoparticles was compared to the combined weight of the polymer and drug to calculate the yield of nanoparticles. Three replicates of individual values were determined, and their mean values were reported.

$$\% \text{ Yield} = \frac{\text{Total amount of PFD NPs}}{\text{Amount of drug} + \text{Polymer}} \times 100$$

### In vitro drug release study

The *in-vitro* drug release tests were carried out on all formulations. A previously estimated and weighed amount of dried CS NPs of Pirfenidone (20 mg) in 100 ml of phosphate buffer saline (PBS) solution pH 7.4 was used to assess pirfenidone release at 37 °C. The drug release technique was studied using a dialysis membrane with a molecular weight cut-off of 12 kDa. The nanoparticles were placed in a dialysis bag and placed in a USP type I dissolution device basket. The dissolution system was maintained at 37 ± 0.5 °C and agitated at 100 rpm [17, 19]. At predetermined time intervals, 3 ml of aliquots were withdrawn. The dissolution medium was replaced with a fresh buffer to maintain the total volume. The collected samples were passed through a 0.22 µm filter membrane and evaluated for the concentration of drug released by UV–Visible spectrophotometer (UV-1700 Pharma Spec, Shimadzu) at 311 nm. The F1 formulation (blank) was replaced by 10 mg of pure PFD powder.

### Kinetic study

The results of an *in vitro* drug release studies of nanoparticles were fitted with various kinetic equations such as zero-order (cumulative percent release vs. time), first-order (log percent drug remaining vs. time), and Higuchi's model (cumulative percent drug release vs. square root of time) to estimate the kinetic and mechanism of drug release. For the linear curve generated by regression analysis,  $R^2$  and  $k$  values were determined. The most appropriate model having the highest  $R^2$  value and least sum of square residuals (SSR) was selected for describing the drug release mechanism [27].

### Accelerated stability study

The accelerated stability study followed the requirements set forth by the International Council for Harmonization. The stability of produced nanoparticles of pirfenidone was tested by storing the optimized formulation in a stability chamber for 180 days at 25 ± 2 °C with a relative humidity of 60 ± 5% and 40 ± 2 °C with a relative humidity of 75 ± 5%. The samples were examined for particle size, zeta potential, polydispersity index, % entrapment efficiency, and drug release at 8 h and 12 h, and any

changes in their physical appearance after a time period of 0, 1, 2, 3, and 6 months [27].

### Formulation of the dry powder inhaler

Initially flow property of PFD nanoparticles was determined. To increase the flow property, PFD nanoparticles and anhydrous inhalable grade lactose were mixed (1:1) manually using geometrical dilution process. The angle of repose, Carr's index and Hausner ratio were carried out of inhalable grade lactose and optimized batch mixture (dry powder inhaler) for the excellent flow property. The optimized formulation further characterized the zeta size and potential to check the changes of nanoparticles in the form of DPI [28, 29].

### In vitro lung deposition study

Cascade impactors are able to define the particles' aerodynamic characteristics by the separation of the dose by the equipment's impactor plates. The use of impactors will predict the deposition of the inhaled particles in the human lung since the deposition of these particles in the human respiratory tract is dependent on the particle's aerodynamic size. Using a nonviable eight-stage Anderson Cascade Impactor (ACI, Thermo Fisher Scientific, Waltham, Massachusetts, USA), the mass median aerodynamic diameter (MMAD) of the pirfenidone NPs was determined as a dry powder inhaler (DPI). The nanoparticles were aerosolized as a DPI with a flow rate of 28 L/min through the cascade impactor. After DPI was deposited in each chamber, the PFD content was measured, dissolved in methanol, and assessed using a UV–Visible spectrophotometer at 311 nm. The mean mass aerodynamic diameter (MMAD), geometric standard diameter (GSD), and percent fine particle fraction (FPF) was calculated using the "MMADCALCULATOR".

## Results

### Influence of various processing parameters on particle size Influence of chitosan concentration

The influence of polymer content in the organic phase on particle size is shown in Fig. 1. The diameter of nanoparticles gradually increases as the concentration of polymer in a constant volume of organic solvent increases. The viscosity of the emulsion increases as the polymer content increases, resulting in a larger emulsion droplet size. In the organic phase, viscous forces resist shear stresses, and the ultimate particle size and size distribution are determined by the total shear stress available for droplet breakdown [30]. The role of polymer concentration in regulating the particle size obtained by the general emulsification process.

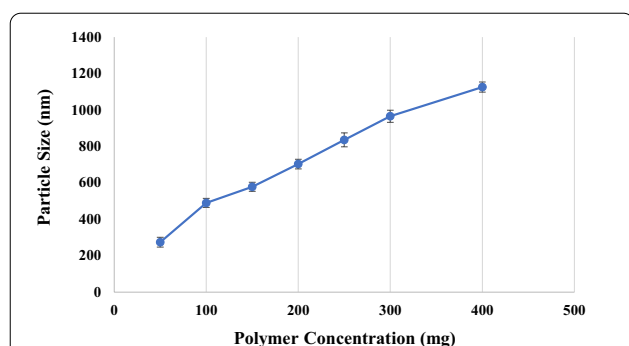


**Fig. 1** Influence of chitosan concentration on the particle size

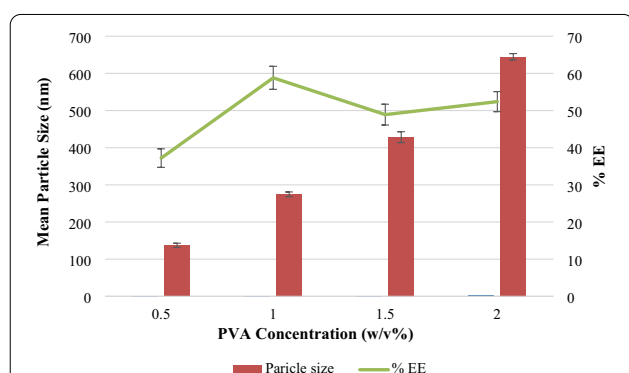


**Fig. 2** Influence of PVA (stabilizer) concentration on the particle size and % EE

#### ***Influence of PVA concentration in the aqueous phase***

From the studies, it was shown that by increasing the stabilizer (PVA) concentration from 0 to 2%, particle size increases continuously. The PFD concentration (100 mg) and chitosan concentration (100 mg) were taken constantly for all batches. The volume of the aqueous phase was taken as constant with modification by increased stabilizer concentration. The PVA effect is obtained as a stabilizer as well as an emulsifying agent in the emulsion. Nanoparticles will form if the stabilizer persists at the liquid–liquid interface during the diffusion process and its protective action is enough. The results are shown in Fig. 2.

The effects of PVA content in the aqueous phase on particle size are shown in Fig. 2. Because of the high aqueous phase viscosity, when the PVA concentrations increase, the particle size steadily increases, reducing the total shear stress accessible for droplet breakdown. Swelling behavior was increased with the increasing concentration of polyvinyl alcohol [31]. The increased concentration of hydroxyl groups in the PVA as the concentration of PVA increases which directly effect on pirfenidone binding proportion.

As an increase in PVA concentration in the aqueous phase, the particle size increases due to more stabilizer molecules are adsorbed on the surface of emulsion droplets, and resulting in larger emulsion droplets formed after solvent evaporation [32]. The entrapment efficiency was observed frequently and as per the result obtained, 1% PVA was observed highest % EE. Only a little amount of stabilizer is absorbed in the emulsion droplet contact. The excess stays in the continuous aqueous phase and has no effect on the emulsification process.

#### **Compatibility study**

##### **FTIR spectroscopy**

In the FTIR spectrum of CS (Fig. 3A), the peaks attributed to  $\text{--OH}$  stretching were found at  $3400\text{ cm}^{-1}$ . The bonds were in the range of  $2886\text{--}2974\text{ cm}^{-1}$  according to the stretching of  $\text{--CH}$ ,  $\text{--CH}_2$ , and  $\text{--CH}_3$ . The amide I and II vibrations, respectively, were found at  $1676\text{ cm}^{-1}$  and  $1600\text{ cm}^{-1}$ .  $\text{N--H}$  stretching vibration was ascribed to the bonds between  $924\text{ cm}^{-1}$  and  $1169\text{ cm}^{-1}$ . The FTIR spectrum of pirfenidone (Fig. 3B), the  $\text{O=C}$  stretch ( $\alpha$ ,  $\beta$  unsaturated ketone) peak observed at  $1612\text{ cm}^{-1}$  and  $\text{C--C}$  Aromatic Stretching Vibration peak was obtained at  $1530\text{ cm}^{-1}$ . The aliphatic Stretching Vibration of  $\text{C--H}$  was found at  $3054\text{ cm}^{-1}$ ,  $\text{C--N}$  aromatic stretch Vibration ( $3^\circ$  amine) was found at  $1274\text{ cm}^{-1}$  and  $\text{C=C}$  phenyl Stretching Vibration at  $825\text{ cm}^{-1}$ .

The surface chemical composition of CS NPs and CS chains was investigated using FTIR spectra (Figs. 4 and 3B). Pirfenidone nanoparticles (optimized batch) were subjected to FTIR analysis. The wiggling of the  $\text{NH}_2$  bond causes the PFD NPs peak to shift to  $1576\text{ cm}^{-1}$ , and the strong peak at  $1412\text{ cm}^{-1}$  is caused by the alkyl group  $\text{C--H}$  bending vibration (Fig. 4). The ionic interaction with the treated molecules indicates the conversion of chitosan polymer in the nano form that forms a cross-link with the treated molecules.

The CS the peaks in the PFD NPs with stretching of  $\text{--CH}$ ,  $\text{--CH}_2$ , and  $\text{--CH}_3$  bonds were observed in the range of  $2885\text{--}2910\text{ cm}^{-1}$ , and  $\text{--OH}$  stretching was found at  $3504\text{ cm}^{-1}$ . The aliphatic Stretching Vibration of  $\text{C--H}$  was found at  $2970\text{ cm}^{-1}$ ,  $\text{C--N}$  aromatic stretch Vibration ( $3^\circ$  amine) was found at  $1280\text{ cm}^{-1}$  and  $\text{C=C}$  phenyl Stretching Vibration at  $842\text{ cm}^{-1}$ . The amide I and II vibrations were found in the PFD NPs at  $1662\text{ cm}^{-1}$  and  $1609\text{ cm}^{-1}$ .  $\text{N--H}$  stretching vibration was ascribed to the bonds between  $962\text{ cm}^{-1}$  and  $1147\text{ cm}^{-1}$ . The FTIR spectrum of PFD loaded NPs;  $\text{C--C}$  Aromatic Stretching Vibration peak obtained  $1550\text{ cm}^{-1}$ . This data is complying that the FTIR spectra peaks of CS and PF were obtained in the PFD loaded CS NPs. There are no peaks are dissolve and resulting that PFD and CS being compatible with the nanoparticle formulation.

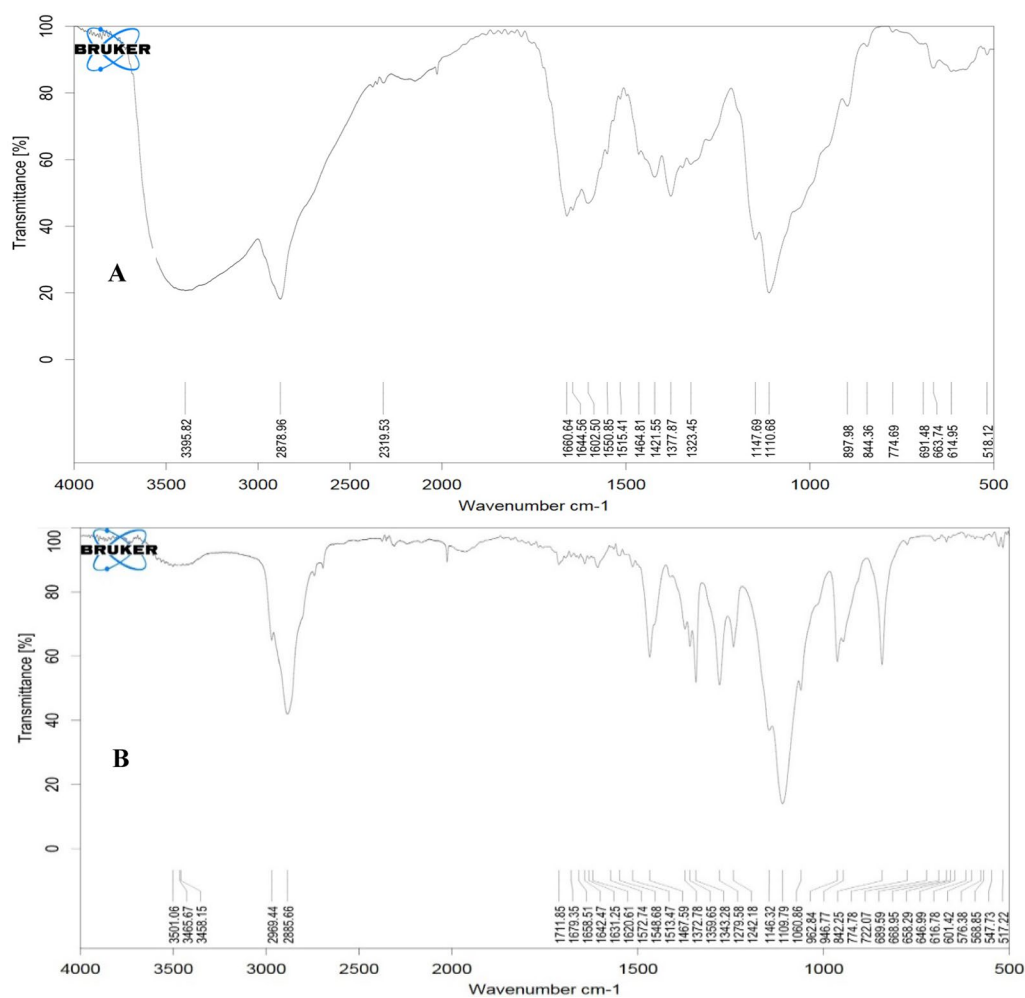


**Fig. 3** FTIR spectra of **A** Chitosan **B** Pirfenidone

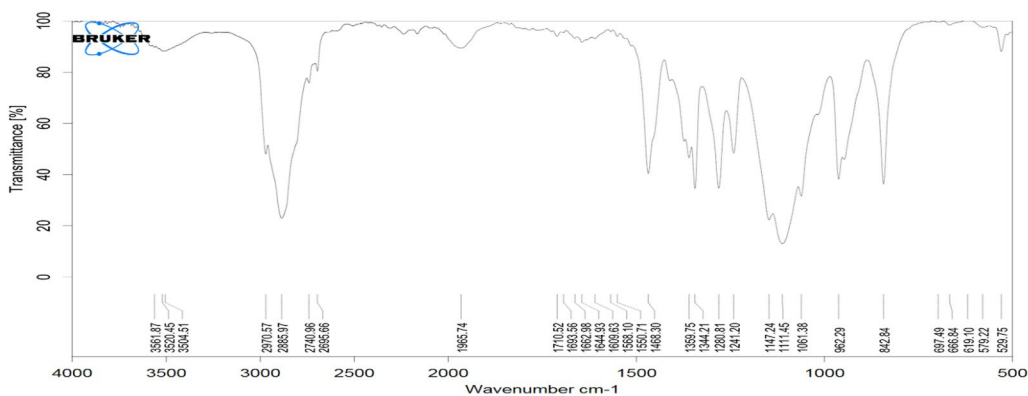


**Fig. 4** FTIR study of pirfenidone loaded chitosan nanoparticles (optimized batch)

#### DSC analysis studies

The standard peak of pirfenidone was observed at 109 °C and the pirfenidone sample peak was observed at around

108.4 °C. The DSC curve of chitosan shows an exothermic peak observed at around 72 °C and an endothermic peak observed at around 311 °C. The DSC curve

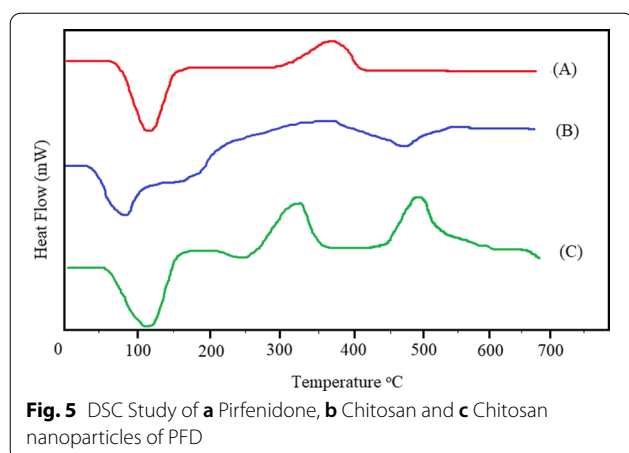


**Fig. 5** DSC Study of **a** Pirfenidone, **b** Chitosan and **c** Chitosan nanoparticles of PFD

of chitosan nanoparticles (Fig. 5) has a wide exothermic peak between 60 °C and 150 °C which is due to the removal of absorbed water and a sharp endothermic peak at 320 °C and 500 °C associated with the breakage of chitosan phosphoric acid cross-linkage [33].

#### Solubility and standard curve of pirfenidone

Pirfenidone is sparingly soluble in water at 25 °C (19 mg/ml) and at 37 °C (21 mg/ml). It is freely soluble in organic solvents such as acetone, ethyl acetate, dichloromethane (DCM), and chloroform at 25 °C. It is very soluble in ethanol [25].

Pirfenidone UV absorption spectra in methanol showed a shoulder peak at 222 nm and a  $\lambda_{\text{max}}$  at 311 nm. The wavelength with the highest absorbance at 311 nm, was chosen for the absorbance measurement [34]. The Beer's range was found to be in the range of 10 to 50  $\mu\text{g}/\text{ml}$  of pirfenidone by using a UV-Visible spectrophotometer (Fig. 6a, b). The variability in the precision study was found within limits proving the method to be precise. Linearity of standard curves was found to be 0.997, 0.999, 0.998, 0.998, and 0.999, respectively. The UV absorption spectra of PFD in pH 7.4 PBS also showed the  $\lambda_{\text{max}}$  at 311 nm.

#### Evaluation of chitosan nanoparticles of PFD

The increase in chitosan concentration, which is explained by enhanced crosslinking responsible for the increased size of formed particles. Improved solubility and dispersion of chitosan NPs are due to the significant influence of acetic acid concentration on NP size. The size of NPs was negatively affected by increasing the stirring speed. When the stirring speed was raised from 800 to 1200 RPM, the particle size decreased from  $584.9 \pm 9.89$  nm to  $218.4 \pm 5.28$  nm. Increased

mechanical shear at higher stirring speeds is thought to be the reason for this reduction in particle size.

#### Particle size

The spherical particles were formed of pirfenidone nanoparticles by using low molecular weight chitosan with solvent evaporation method of preparation. The particle size is affected by the incorporation of the organic solvent containing PFD into chitosan solution with polyvinyl alcohol under a magnetic stirrer. The mean particle size ranged from  $239.3 \pm 1.8$  nm to  $928.7 \pm 4.6$  nm as seen in Table 1. Particle size was highly influenced by chitosan concentration and molecular weight (medium and high molecular weight). Higher chitosan concentration produced larger nanoparticles due to larger droplet size formation during emulsification [35]. F2 formulation (50 mg chitosan) had the smallest particle size as compared to the F7 formulation (300 mg).

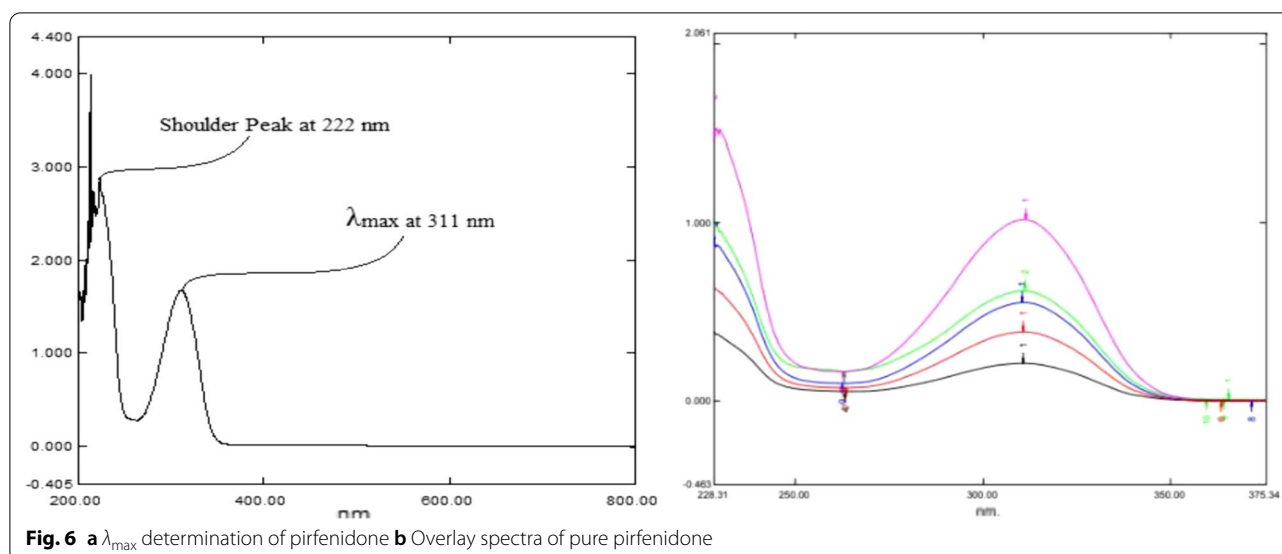
#### Zeta potential

The zeta potential was observed to be directly proportional to the concentration of chitosan used in the formulation of nanoparticles. The zeta potential was found in the range of  $32.5 \pm 1.4$  mV to  $38.9 \pm 1.0$  mV shown in Table 1. This indicates that the surfaces of the nanoparticles were primarily made up of chitosan. It's also critical that positively charged nanoparticles interact easily with negatively charged cell membranes and be easily released. The formation of positively charged chitosan NPs is suggested by the positive zeta potential values [35, 36]. The net positive charge of NPs is an unavoidable condition for electrostatic interaction with negatively charged sialic acid on the surface of alveolar macrophages, which benefits in increased absorption of PFD-loaded NPs by these cells.

#### Polydispersity index (PDI)

Nanoparticles with PDI smaller than 0.4 has to be considered acceptable for drug delivery of nanoparticles to a deep pulmonary region (alveoli) according to some references. The term "polydispersity" is used to describe the degree of non-uniformity of size distribution of particles. The PDI of pirfenidone nanoparticles by solvent evaporation method was found to be  $0.1214 \pm 0.062$  to  $0.481 \pm 0.022$  range (Table 1). As the PDI value increases, the heterogeneity in cross-linking, network formation, chain length, branching, and hyper branching will be more with more random arrangement [37].



**Table 1** Formulation and physicochemical evaluation of pirfenidone nanoparticles

Batch	Drug (mg)	CS (mg)	MPS (nm)	ZP (mV)	Charge	PDI	% Yield	% EE	% DR <sub>8</sub>	% DR <sub>12</sub>
F1	0	100	239.3 ± 1.8	35.0 ± 1.2	strongly cationic	0.181 ± 0.010	56	0	—	—
F2	100	50	248.6 ± 1.4	32.5 ± 1.4	strongly cationic	0.191 ± 0.012	60	17.00 ± 2.0	92.15 ± 2.04	98.94 ± 2.49
F3	100	100	440.8 ± 3.9	36.3 ± 0.8	strongly cationic	0.121 ± 0.062	55.5	23.76 ± 1.8	86.53 ± 3.04	95.25 ± 2.89
F4	100	150	549.1 ± 0.3	37.7 ± 1.4	strongly cationic	0.205 ± 0.023	56.33	34.98 ± 4.7	84.21 ± 2.53	92.34 ± 2.49
F5	100	200	687.8 ± 4.3	34.4 ± 1.8	strongly cationic	0.240 ± 0.030	51.33	39.60 ± 4.0	82.43 ± 1.49	90.21 ± 1.35
F6	100	250	803.4 ± 2.6	35.7 ± 0.5	strongly cationic	0.344 ± 0.024	59.33	61.20 ± 7.0	81.67 ± 1.36	87.66 ± 1.36
F7	100	300	928.7 ± 4.6	38.9 ± 1.0	strongly cationic	0.481 ± 0.022	54.33	60.48 ± 4.3	79.78 ± 2.47	85.36 ± 2.16

Mean particle size (nm), Polydispersity index (PDI), Zeta Potential (mV), % Drug entrapment efficiency (EE), % Drug Release at 8 h., and % Drug Release at 12 h.  
Mean ± SD. N=3

### Yield of nanoparticles

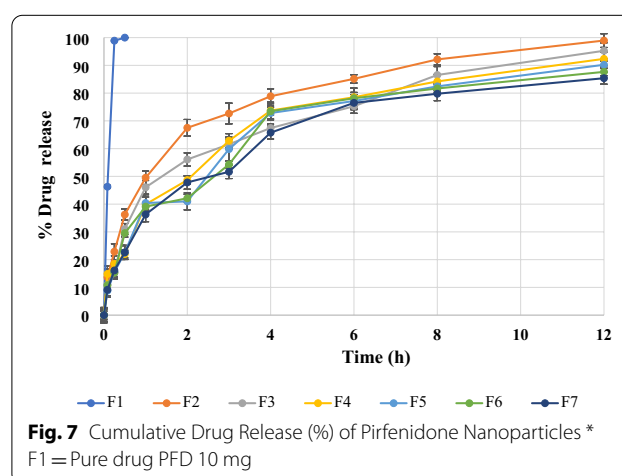
The % yield of chitosan nanoparticles was found to be in the range of 51.33 to 60% for all prepared batches shown in Table 1. Drug particles were wasted less but the pirfenidone is solubilizing in water and the drug entrapment reduces. That reduces the nanoparticles to 60%. The sonication time directly affects the % yield due to the drug was more and more solubilize under sonication and the % output of nanoparticles is reduced with % yield.

### % Entrapment efficiency

The drug entrapment efficiency of nanoparticles containing drug: polymer in various ratios of 1:0.5, 1:1, 1:1.5, 1:2, 1:2.5 and 1:3 was found to be 17.00 ± 2.0, 23.76 ± 1.8, 34.98 ± 4.7, 39.60 ± 4.0, 61.20 ± 7.0, 60.48 ± 4.3% respectively (Table 1). As a result, increasing the polymer content in the formulation resulted in a continuous increase in entrapment efficiency. The high entrapment efficiency is likely due to electrostatic interactions between the drug and the polymer.

### Drug release of CS-PFD-NPs

Pirfenidone NPs were tested in vitro for drug release characteristics. The release pattern of PFD from Chitosan nanoparticles was evaluated using phosphate



buffer saline with a pH of 7.4 and a temperature of 37 °C. The release curve given in Fig. 7 shows the drug release of pure drug pirfenidone (F1) 10 mg was found to be 99.99% within the first sampling. The initial burst release of PFD-Chitosan nanoparticles was 21%, and the release rate increased to  $95.25 \pm 2.89\%$  in 12 h as per shown in Table 1. This initial burst release would aid in improving the target plasma concentration in the lungs, while the sustained release would aid in maintaining the dose for a longer length of time. Drug release from drug-associated relatively close particle surfaces that may have been removed when they came into contact with the dissolving medium [22, 38]. The formulations manufactured using the evaporation approach, on the other hand, finished product releasing pirfenidone in 12 h. This is due to the differences in formulation procedures as well as particle structure. The encapsulation of pirfenidone with electrostatic powers is more condensed in the solvent evaporation approach. The pirfenidone release period becomes prolonged due to that reason.

### Drug release kinetic study

The corresponding dissolving data were fitted into various kinetic dissolution models, such as Zero order, First order, and Higuchi, and Korsmeyer Peppas plots to describe the release kinetics of all six formulations (Table 2). The drug release from all formulations follows first-order release and the Higuchi model, as demonstrated by greater  $R^2$  (coefficient of correlation) values.

### Optimized batch evaluation

#### Composition and evaluation of the optimized batch

The optimized formulation had the 100 mg of PFD added in the organic phase containing DCM and 100 mg of chitosan was added in the 20 ml of aqueous phase containing 1% stabilizer (PVA) solution. The organic phase was added to the aqueous phase with continuous stirring and other procedures were followed as per mention above as preparation of PFD NPs. The optimization of the formulation was done with the different parameters like mean particle size ( $467.33 \pm 7.8$  nm), zeta potential ( $34.8 \pm 1.6$  mV), surface charge (strongly cationic),

polydispersity index ( $0.127 \pm 0.022$ ), % entrapment efficiency ( $39.45 \pm 4.63$ ), and % drug release after 12 h ( $94.78 \pm 2.88$ ). The optimized formulation was further converted into the inhalable free-flowing powder for ease of application [39].

### Scanning electron microscopy (SEM)

The surface morphological structure was further examined by SEM analysis. SEM images of optimized formulation showed that the nanoparticles were spherical in shape and particles in the agglomerated state (Fig. 8). Furthermore, the size uniformity of the nanoparticles is shown. Most of the particle size was found to be  $501.9 \pm 16.8$  nm, which is suitable for the inhalation formulation. The particle size of a PFD formulation intended for inhalation, together with the particle density, is an important factor in the formulation's effectiveness since it affects the powder's dispersion and sedimentation properties. The rest of the cases aggregation occurred due to moisture entrapment during handling.

### Characterization of dry powder inhaler

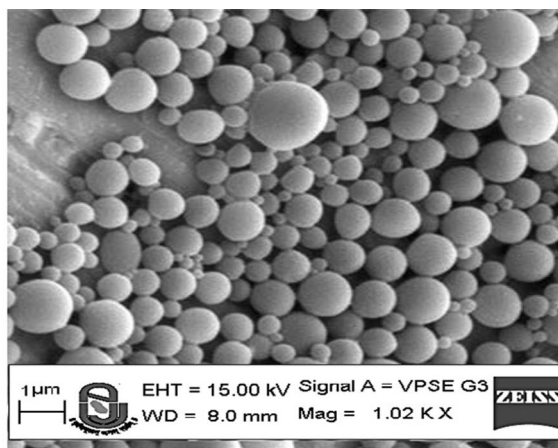
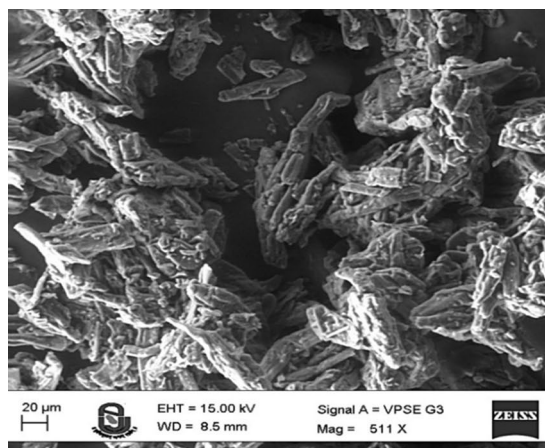
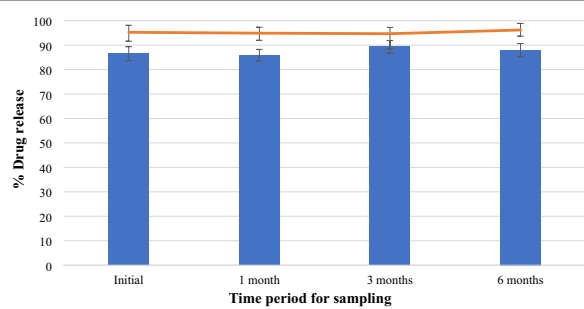
The fluffy mass of freeze-dried nanoparticles has a fair flow property. The Carr's index, Hausner ratio, and angle of repose of these nanoparticles were 18.12%, 1.23, and  $36.44^\circ$  respectively. To improve the bulk and flow properties of nanoparticles, special inhalable grade lactose was applied. The flow quality of this specific grade of lactose was greatly improved due to the small particles. The proportion of 1:1 ratio of anhydrous lactose was added to the optimized PFD NPs by physical geometric mixture. The Carr's index, Hausner ratio, and angle of repose of these nanoparticles were  $10.67 \pm 1.3\%$ ,  $1.11 \pm 0.01$ , and  $26.42 \pm 1.87^\circ$  respectively. For the produced DPI containing PFD NPs, zeta analysis was performed, and no significant alterations in zeta potential were found. To improve the bulk and flow properties of nanoparticles, special inhalable grade lactose was applied. Due to fine particles of this special grade lactose, flow property was increased significantly.

**Table 2** Correlation coefficients according to different kinetic equations

Formulation	% Drug release	Zero order	First order	Higuchi plot	Peppas plot	'n' Value
F1	99.99	—	—	—	—	—
F2	98.94	0.749	0.992	0.959	0.989	0.387
F3	95.25	0.930	0.979	0.918	0.974	0.478
F4	92.34	0.785	0.978	0.917	0.968	0.393
F5	90.21	0.862	0.956	0.975	0.997	0.369
F6	87.66	0.748	0.988	0.971	0.978	0.377
F7	85.37	0.789	0.987	0.889	0.983	0.402

**Table 3** Stability study of optimized batch pirfenidone nanoparticles

Evaluation parameter	Time period for sampling			
	Initial	After 1 month	After 3 months	After 6 months
Particle size (nm)	440.8 ± 3.9	459.3 ± 3.8	459.3 ± 3.8	459.3 ± 3.8
Zeta potential (mV)	36.3 ± 0.8	37.7 ± 1.13	36.78 ± 2.01	40.4 ± 2.51
% Entrapment efficiency	32.76 ± 1.8	33.11 ± 1.39	34.26 ± 1.69	31.6 ± 1.28
PDI	0.121 ± 0.032	0.129 ± 0.052	0.123 ± 0.041	0.137 ± 0.071
% drug release at 8 h	86.53 ± 3.45	85.83 ± 1.87	89.32 ± 2.14	87.96 ± 2.01
% drug release at 12 h	95.25 ± 2.84	94.89 ± 1.66	94.67 ± 2.16	96.19 ± 1.86

**Fig. 8** a Surface morphology using SEM of raw pirfenidone drug powder b Surface morphology using SEM of pirfenidone nanoparticles (optimized batch)**Fig. 9** Stability study for cumulative % drug release study of pirfenidone nanoparticles

### Stability study

Stability studies showed that pirfenidone nanoparticles using chitosan as a polymer was stable after six months when stored at 25 °C and 40% relative humidity as per ICH guidelines and retained their initial size, zeta potential, Polydispersity index, % entrapment efficiency, and cumulative % drug release after 8 h and 12 h found stable

as per shown in Table 3 and Fig. 9 data. There was no major change in physical properties was observed and no significant aggregation of particles occurred during the storage period. The formulated PFD-loaded chitosan nanoparticles are stable for and not aggregated for six-month stability study.

### In-Vitro drug deposition by andersen cascade impactor (ACI)

Particles targeting the deep lung should be fine enough to enter via the mouth, throat, and conducting airways, but not so small that they fail to deposit and are exhaled out again. As a result, their aerodynamic diameter should be between 1 and 5 µm. Even so, mucociliary clearance will move a certain quantity of particles away from the lungs [40]. The eight-stage Anderson Cascade Impactor (ACI, Thermo Fisher Scientific Inc.) was used to determine the mass median aerodynamic diameter (MMAD) of dry powder inhaler nanoparticles of pirfenidone. The deposition of PFD-loaded DPI in the different chambers of the cascade impactor was evaluated using HPLC based on particle size. Extra fine particle fraction and Fine particle

fraction were found at 16.92% and 81.49% respectively. The emitted dose from the sample device Rotahaler was found to be 96.37%. The aerodynamic particle size of optimized nanoparticles was 1.28  $\mu\text{m}$ , with a geometric standard deviation of 2.46. As a result, Prepared DPI can reach deep into the lungs.

## Discussion

The purpose of this research was to create an optimal nanoparticulate composition that could be delivered through the lungs. It was also envisaged that the formulation would be kept in the target organ (lungs) for a longer period of time, resulting in a larger medication concentration. The average particle size and polydispersity index were sought to be optimized in order for the nano-formulation to be efficiently administered to the lungs via the inhalation route, allowing for increased retention in the lungs for a longer period of time. Physical stability was also important before the nanoparticle dispersion was lyophilized. As a result, the zeta potential was deemed crucial.

Spherical nanoparticles were formed spontaneously upon the incorporation of pirfenidone in DCM solution to the chitosan solution under magnetic stirring. In this study, a new hydrophilic dry powder containing pirfenidone-loaded nanoparticles was created using quasi-emulsion solvent evaporation, which is a simple process that involves several processing and materials parameters, including the amount and duration of energy utilized, the volume of the aqueous phase, the concentration of polymer and drug in the organic phase, the molecular weight of the polymer, the polymer end groups, the solvent volume, and the surfactant concentration. To assist the formulation of NPs, an organic phase and an aqueous phase was required in this emulsion. Following organic solvent diffusion, nanoparticles are formed by colliding and consolidating emulsion droplets, and their size is determined by the stability of the emulsion droplets. All of these techniques and material properties have an impact on the size and/or drug content of nanoparticles. Even though DCM is immiscible with water, practically every nanoparticulate formulation that used it as the organic phase solvent resulted in significant aggregation and large mean particle size. DCM formulations were more effective in entrapping PLGA nanoparticles and were preferred. Despite the presence of a stabilizer, acetone and ethanol are completely miscible in water and do not form stable emulsions. The PLGA creates sub-micron particles when the two phases are mixed, resulting in large particle size due to the coalescence of droplets formed in an emulsion containing acetone or ethanol as an organic phase.

We found that the total polymer concentration affected the particle size. The higher the concentration

of chitosan favored the formation of larger particles due to the more complex and large formation of the polymer matrix. The polymer concentration was also affected by the amount of PFD entrapment, for that as the increased CS concentration were increases particle size. We had selected 100 mg of chitosan for the optimized formulation which had a small enough particle size to suggested pulmonary delivery. Nanoparticles have been used to increase drug uptake and activity in the lungs, and it is well known that smaller nanoparticles cross the surfactant layer more readily than bigger nanoparticles, owing to reduced steric hindrance.

The particle size is expected to decrease as the surfactant concentration is increased. The opposite effects were found and explained by particle aggregation caused by the surfactant's bridging effect. Entrapment efficiency is influenced by surfactant content as well. Entrapment efficiency was reduced as surfactant content was increased. These phenomena could be caused by an electrostatic contact or repulsion between the surfactant and the medication. Another explanation for this phenomenon is an increase in pirfenidone solubility in the aqueous phase in the presence of high surfactant concentrations, leading it to diffuse into the aqueous environment and lowering entrapment efficiency.

The zeta potential value can also be used to predict particle physical stability. The presence of a zeta potential over +30 mV and/or below -30 mV suggests that the particles are colloiddally stable. The charge density on the surface of chitosan nanoparticles has been demonstrated to be dependent on the nanoparticle size and the amount of chitosan employed in the synthesis. The quantity of free amine groups is expected to increase as the amount of chitosan employed in the manufacture of the NPs increases, resulting in increased zeta potentials. The influence of particle size on the zeta potential, on the other hand, is more complicated. The total surface area per weight of any given sample increases with the size of the particles, whereas the individual particles have decreasing surface areas. As a result, the zeta potentials grew as the size of the chitosan NPs increased until they reached a maximum value.

The release mechanism was swelling, and diffusion controlled since it was validated as a Higuchi model. The Peppas model is frequently used to determine if a release mechanism is a Fickian diffusion, non-Fickian diffusion, or zero-order diffusion. The value of ' $n$ ' (Korsmeyer-Peppas model release exponent) can be used to characterize distinct release mechanisms [41]. For all formulations, the ' $n$ ' values were found to be smaller than 0.50. This means the release is close to a fickian diffusion mechanism.



The PFD nanoparticles were aerodynamically characterized “in vitro” and its ability to deliver the nanoparticles was investigated; thus, demonstrating its potential for pulmonary administration of pirfenidone for idiopathic pulmonary fibrosis. The low molecular weight of chitosan influences encapsulation of active material efficiency and in vitro release properties. The degree of deacetylation of chitosan affects many inherent qualities of the polymer itself such as, solubility, degradation rate, efficiency of pulmonary administration, and stability of particle size.

The design of an acceptable carrier system has become a requirement for deep lung delivery and selecting one for NP delivery is still difficult. Apart from the required safety when it comes to contact with lung tissue, the carrier should also provide the convenience of handling during filling and processing, drug stability, suitable aerodynamic qualities for proper lung deposition, and increased powder flowability to improve drug dispersion from the inhaler device [42].

## Conclusions

The pirfenidone nanoparticles were prepared successfully by a quasi-emulsion solvent evaporation method and evaluated based on mean particle size, zeta potential, polydispersity index, surface morphology, % entrapment efficiency, drug release at 24 h, kinetic study, stability study, in vitro drug deposition study. The optimized formulation having a mean particle size of  $440.8 \pm 3.9$  nm;  $36.3 \pm 0.8$  mV zeta potential with cationic surface charged;  $32.76 \pm 1.8\%$  entrapment efficiency, % drug release of  $95.25 \pm 3.64\%$  at 12 h. The spherical smooth surface was observed from SEM images. The aerodynamic study showed MMAD of  $1.28 \mu\text{m}$  indicating that PFD NPs can penetrate deep into the lungs for effective treatment of idiopathic pulmonary fibrosis. Further, release kinetic studies can be conducted to evaluate that release approximates the fickian diffusion mechanism the stability study of optimized batch revealed that the pirfenidone nanoparticles using chitosan as polymer was stable after a six-month study as per ICH guideline. To target idiopathic pulmonary fibrosis, this nanoparticle can improve the efficiency of the treatment by enhancing pirfenidone concentration in the deep lungs tissue with a single and lower dose.

## Abbreviations

MMAD: Mass median aerodynamic diameter; IPF: Idiopathic pulmonary fibrosis; PFD: Pirfenidone; FPF: Fine particle fraction; CS: Chitosan; PVA: Polyvinyl alcohol; DCM: Dichloromethane; NPs: Nanoparticles; FTIR: Fourier-transform infrared spectroscopy; DSC: Differential scanning calorimetry; SEM: Scanning electron microscopy; PBS: Phosphate buffer saline; SSR: Sum of square residuals; ACI: Anderson cascade impactor; DPI: Dry powder inhaler; GSD: Geometric standard diameter; MPS: Mean particle size; PDI: Polydispersity index; ZP: Zeta potential; % EE: % Entrapment efficiency; % DR<sub>8</sub>: % Drug release at 8 h; % DR12%: Drug release at 12 h.

## Acknowledgements

All authors have read and approved the final manuscript. The authors are thankful to Meck Pharmaceuticals & Chemicals Private Limited and ZCL Chemicals Ltd., Gujarat, India for providing respective gift samples. The authors would like to thank Dr. Praful Bharadiya, Dr. Mihir Raval, and Dr. Dhaval Mori for their helpful comments.

## Author contributions

All authors have read and approved the final manuscript. The authors, Ms. Kiran Dudhat are considerably subsidized to the writing of this research article. Development, Design, and evaluation of the PFD-loaded chitosan nanoparticles were by Ms. Kiran Dudhat. Dr. Harsha Patel, who guide and reviewed the article judgmentally for its knowledgeable content and assisted in the concluding endorsement of the version to published.

## Funding

We received minor research grant from Student Startup and Innovation Policy, Government of Gujarat, India, and KS Patel Centre for Entrepreneurship, RK University Rajkot. Application number RKU/SOP/21/2/7.

## Availability of data and materials

Data and materials are available upon request.

## Declarations

### Ethics approval and consent to participate

No any animal or human were used during this experimental study.

### Consent for publication

The research work embodied in this article is original research work of me and my team. It is neither published nor being considered for publication elsewhere. On behalf of all the authors, I will act and guarantor and will correspond with the journal from this point onward.

### Competing interests

The author declares that they have no competing interests.

### Author details

<sup>1</sup>Department of Pharmaceutics, School of Pharmacy, R K University, Kasturbadham, Rajkot, Gujarat 360020, India. <sup>2</sup>Gujarat Technological University, Chandkheda, India. <sup>3</sup>Indukaka Ipcowala College of Pharmacy, New Vallabh Vidyanaga, Vitthal Udyognagar, Anand, Gujarat 388121, India.

Received: 13 January 2022 Accepted: 9 May 2022

Published online: 03 June 2022

## References

- King TE Jr, Pardo A, Selman M (2011) Idiopathic pulmonary fibrosis. The Lancet 378(9807):1949–1961. [https://doi.org/10.1016/S0140-6736\(11\)60052-4](https://doi.org/10.1016/S0140-6736(11)60052-4)
- Dudhat KR, Patel HV (2020) Novel nanoparticulate systems for idiopathic pulmonary fibrosis: a review. Asian J Pharm Clin Res 13(11):3–11. <https://doi.org/10.22159/ajpcr.2020.v13i11.39035>
- Richeldi L, Collard HR, Jones MG (2017) Idiopathic pulmonary fibrosis. Lancet 389(10082):1941–1952. [https://doi.org/10.1016/S0140-6736\(17\)30866-8](https://doi.org/10.1016/S0140-6736(17)30866-8)
- Martinez FJ, Safrin S, Weycker D et al (2005) The clinical course of patients with idiopathic pulmonary fibrosis. Ann Intern Med 142(12\_Part\_1):963–967. [https://doi.org/10.7326/0003-4819-142-12\\_part\\_1-200506210-00005](https://doi.org/10.7326/0003-4819-142-12_part_1-200506210-00005)
- Ley B, Collard HR (2013) Epidemiology of idiopathic pulmonary fibrosis. Clin Epidemiol 5:483. <https://doi.org/10.2147/CLEP.S54815>
- Collard HR, Moore BB, Flaherty KR et al (2007) Acute exacerbations of idiopathic pulmonary fibrosis. Am J Respir Crit Care Med 176(7):636–643. <https://doi.org/10.1164/rccm.200703-463PP>
- Gross TJ, Hunninghake GW (2001) Idiopathic pulmonary fibrosis. N Engl J Med 345(7):517–525. <https://doi.org/10.1056/NEJMra003200>

8. Adamali HI, Maher TM (2012) Current and novel drug therapies for idiopathic pulmonary fibrosis. *Drug Des Devel Ther* 6:261–272. <https://doi.org/10.2147/DDDT.S29928>
9. Nathan SD, Albera C, Bradford WZ et al (2017) Effect of pirfenidone on mortality: pooled analyses and meta-analyses of clinical trials in idiopathic pulmonary fibrosis. *Lancet Respir Med* 5(1):33–41. [https://doi.org/10.1016/S2213-2600\(16\)30326-5](https://doi.org/10.1016/S2213-2600(16)30326-5)
10. Taniguchi H, Ebina M, Kondoh Y et al (2010) Pirfenidone in idiopathic pulmonary fibrosis. *Eur Respir J* 35(4):821–829. <https://doi.org/10.1183/09031936.00005209>
11. Silva RO, da Costa BL, da Silva FR et al (2019) Treatment for chemical burning using liquid crystalline nanoparticles as an ophthalmic delivery system for pirfenidone. *Int J Pharm* 568:118466. <https://doi.org/10.1016/j.ijpharm.2019.118466>
12. Kim ES, Keating GM (2015) Pirfenidone: a review of its use in idiopathic pulmonary fibrosis. *Drugs* 75(2):219–230. <https://doi.org/10.1007/s40265-015-0350-9>
13. Carter NJ (2011) Pirfenidone: in idiopathic pulmonary fibrosis. *Drugs* 71(13):1721–1732. <https://doi.org/10.2165/11207710-000000000-00000>
14. Liu Q, Guan J, Qin L et al (2020) Physicochemical properties affecting the fate of nanoparticles in pulmonary drug delivery. *Drug Discov Today* 25(1):150–159. <https://doi.org/10.1016/j.drudis.2019.09.023>
15. Kumar MR, Muzzarelli RA, Muzzarelli C et al (2004) Chitosan chemistry and pharmaceutical perspectives. *Chem Rev* 104(12):6017–6084. <https://doi.org/10.1021/cr030441b>
16. Mourya V, Inamdar NN (2008) Chitosan-modifications and applications: opportunities galore. *React Funct Polym* 68(6):1013–1051. <https://doi.org/10.1016/j.reactfunctpolym.2008.03.002>
17. Pourshahab PS, Gilani K, Moazeni E et al (2011) Preparation and characterization of spray dried inhalable powders containing chitosan nanoparticles for pulmonary delivery of isoniazid. *J Microencapsul* 28(7):605–613. <https://doi.org/10.3109/02652048.2011.599437>
18. Garg T, Rath G, Goyal AK (2016) Inhalable chitosan nanoparticles as antitubercular drug carriers for an effective treatment of tuberculosis. *Artif Cells Nanomed Biotechnol* 44(3):997–1001. <https://doi.org/10.3109/21691401.2015.1008508>
19. Debnath SK, Saisivam S, Debnath M et al (2018) Development and evaluation of chitosan nanoparticles based dry powder inhalation formulations of Prothionamide. *PLoS ONE* 13(1):e0190976. <https://doi.org/10.1371/journal.pone.0190976>
20. Zhang S, Kawakami K (2010) One-step preparation of chitosan solid nanoparticles by electrospray deposition. *Int J Pharm* 397(1–2):211–217. <https://doi.org/10.1016/j.ijpharm.2010.07.007>
21. Lee M, Cho YW, Park JH et al (2006) Size control of self-assembled nanoparticles by an emulsion/solvent evaporation method. *Colloid Polym Sci* 284(5):506–512. <https://doi.org/10.1007/s00396-005-1413-3>
22. Petkar KC, Chavhan S, Kunda N et al (2018) Development of novel octanoyl chitosan nanoparticles for improved rifampicin pulmonary delivery: optimization by factorial design. *AAPS PharmSciTech* 19(4):1758–1772. <https://doi.org/10.1208/s12249-018-0972-9>
23. Patel BK, Parikh RH, Aboti PS (2013) Development of oral sustained release rifampicin loaded chitosan nanoparticles by design of experiment. *J drug deliv*. <https://doi.org/10.1155/2013/370938>
24. Pandit J, Sultana Y, Aqil M (2017) Chitosan-coated PLGA nanoparticles of bevacizumab as novel drug delivery to target retina: optimization, characterization, and in vitro toxicity evaluation. *Artif Cells Nanomed Biotechnol* 45(7):1397–1407. <https://doi.org/10.1080/21691401.2016.1243545>
25. Kumari N, Bhattacharya B, Roy P et al (2019) Enhancing the pharmaceutical properties of pirfenidone by mechanochemical cocrystallization. *Cryst Growth Des* 19(11):6482–6492. <https://doi.org/10.1021/acs.cgd.9b00932>
26. Parvathaneni V, Kulkarni NS, Shukla SK et al (2020) Systematic development and optimization of inhalable pirfenidone liposomes for non-small cell lung cancer treatment. *Pharmaceutics* 12(3):206. <https://doi.org/10.3390/pharmaceutics12030206>
27. Sharma M, Sharma R, Jain DK et al (2019) Enhancement of oral bioavailability of poorly water soluble carvedilol by chitosan nanoparticles: Optimization and pharmacokinetic study. *Int J Biol Macromol* 135:246–260. <https://doi.org/10.1016/j.jbiomac.2019.05.162>
28. Rawal T, Parmar R, Tyagi RK et al (2017) Rifampicin loaded chitosan nanoparticle dry powder presents an improved therapeutic approach for alveolar tuberculosis. *Colloids Surf B Biointerfaces* 154:321–330. <https://doi.org/10.1016/j.colsurfb.2017.03.044>
29. Wang H, George G, Islam NJAPT (2018) Nicotine-loaded chitosan nanoparticles for dry powder inhaler (DPI) formulations—Impact of nanoparticle surface charge on powder aerosolization. *Eur J Pharm Biopharm* 29(12):3079–3086. <https://doi.org/10.1016/j.ejpb.2016.12.023>
30. Scolari IR, Pérez PL, Musri MM et al (2020) Rifampicin loaded in alginate/chitosan nanoparticles as a promising pulmonary carrier against *Staphylococcus aureus*. *Drug Deliv Transl Res* 10(5):1403–1417. <https://doi.org/10.1007/s13346-019-00705-3>
31. Michailidou G, Ainali NM, Xanthopoulou E et al (2020) Effect of poly (vinyl alcohol) on nanoencapsulation of budesonide in chitosan nanoparticles via ionic gelation and its improved bioavailability. *Polymers* 12(5):1101. <https://doi.org/10.3390/polym12051101>
32. Otraj M, Taymouri S, Varshosaz J et al (2020) Preparation and characterization of dry powder containing sunitinib loaded PHBV nanoparticles for enhanced pulmonary delivery. *J Microencapsul* 56:101570. <https://doi.org/10.3109/02652048.2011.599437>
33. Mandapalli PK, Labala S, Bojja J et al (2016) Effect of pirfenidone delivered using layer-by-layer thin film on excisional wound healing. *Eur J Pharm Sci* 83:166–174. <https://doi.org/10.1016/j.ejps.2015.12.027>
34. Manjusha P, Muthu S, Raajaraman B (2020) Density functional studies and spectroscopic analysis (FT-IR, FT-Raman, UV-visible, and NMR) with molecular docking approach on an antifibrotic drug Pirfenidone. *J Mol Struct* 1203:127394. <https://doi.org/10.1016/j.molstruc.2019.127394>
35. Gan Q, Wang T, Cochrane C et al (2005) Modulation of surface charge, particle size and morphological properties of chitosan-TPP nanoparticles intended for gene delivery. *Colloids Surf B Biointerfaces* 44(2–3):65–73. <https://doi.org/10.1016/j.colsurfb.2005.06.001>
36. Vaezifar S, Razavi S, Golozar MA et al (2013) Effects of some parameters on particle size distribution of chitosan nanoparticles prepared by ionic gelation method. *J Cluster Sci* 24(3):891–903. <https://doi.org/10.1007/s10876-013-0583-2>
37. Fan W, Yan W, Xu Z et al (2012) Formation mechanism of monodisperse, low molecular weight chitosan nanoparticles by ionic gelation technique. *Colloids Surf B Biointerfaces* 90:21–27. <https://doi.org/10.1016/j.colsurfb.2011.09.042>
38. Garg U, Chauhan S, Nagaich U et al (2019) Current advances in chitosan nanoparticles based drug delivery and targeting. *Adv Pharm Bull* 9(2):195. <https://doi.org/10.15171/apb.2019.023>
39. Alhajj N, O'Reilly NJ, Cathcart HJPT (2021) Designing enhanced spray dried particles for inhalation: a review of the impact of excipients and processing parameters on particle properties. *Powder Tech* 384:313–331. <https://doi.org/10.1016/j.powtec.2021.02.031>
40. Chow MYT, Tai W, Chang RYK et al (2021) In vitro-in vivo correlation of cascade impactor data for orally inhaled pharmaceutical aerosols. *Adv Drug Deliv Rev* 11:39–52. <https://doi.org/10.1016/j.addr.2021.113952>
41. Pardeshi CV, Agnihotri VV, Patil KY et al (2020) Mannose-anchored N, N-trimethyl chitosan nanoparticles for pulmonary administration of etofylline. *Int J Biol Macromol* 165:445–459. <https://doi.org/10.1016/j.jbiomac.2020.09.163>
42. Afrose A, White ET, Howes T et al (2018) Preparation of ibuprofen microparticles by antisolvent precipitation crystallization technique: characterization, formulation, and in vitro performance. *J Pharm Sci* 107(12):3060–3069. <https://doi.org/10.1016/j.xphs.2018.07.030>

## Publisher's Note

Springer Nature remains neutral with regard to jurisdictional claims in published maps and institutional affiliations.